Modern Pathology (2004) 17, 1364–1371

www.modernpathology.org

Loss of heterozygosity of chromosome 9p and loss of *p16^{INK4A}* expression are associated with malignant gastrointestinal stromal tumors

Muna Sabah, Robert Cummins, Mary Leader and Elaine Kay

Department of Histopathology, Beaumont Hospital and Royal College of Surgeons in Ireland, Dublin, Ireland

Gastrointestinal stromal tumors GISTs are distinctive KIT-positive mesenchymal neoplasms. The genetic alterations leading to the malignant behavior of these tumors are not well characterized. In this study, 21 cases of GISTs (eight low malignant potential, nine primary malignant and four intra-abdominal recurrences) were characterized by immunohistochemistry and evaluated for loss of heterozygosity of the short arm of chromosome 9, using six microsatellite markers. Loss of heterozygosity with at least one microsatellite marker at 9p region was a common finding in high-risk GISTs (malignant and recurrent group) but was absent in the low malignant potential group. Recurrent GISTs showed more frequent deletions than their primary tumors. All cases with loss of heterozygosity showed deletions at 9p21. Similarly, all low malignant potential GISTs were immunoreactive for p16, whereas malignant tumors were negative for p16. These results suggest that loss of *p16^{INK4A}* gene on 9p may contribute to the progression and/or malignant transformation of GISTs.
Modern Pathology (2004) **17,** 1364–1371, advance online publication, 4 June 2004; doi:10.1038/modpathol.3800199

Keywords: gastrointestinal stromal tumors; KIT; $p16^{INK4A}$; loss of heterozygosity; high-risk GISTs; low malignant potential

Gastrointestinal stromal tumors (GISTs) comprise the largest subset of mesenchymal tumors of the digestive tract. These tumors have been the subject of considerable debate in the literature regarding their histogenesis, criteria for diagnosis, prognostic features and biological behavior.[1–3]

It has been suggested that these neoplasms originate from the interstitial cells of Cajal or from stem cells that differentiate towards the interstitial cells of Cajal.[3,4] Immunohistochemical studies revealed that GISTs have similar features to the interstitial cells of Cajal, being positive with CD34 and KIT and negative or variably positive for other neural and smooth muscle markers.[4] Activating mutation of c-*kit* proto-oncogene leading to constitutive expression of KIT protein is believed to have a role in the tumorigenesis of the majority of GISTs.[5,6] *c-Kit* encodes a transmembrane tyrosine kinase receptor that binds to stem cell factor. This interaction is essential for the development of many cell types including the interstitial cells of Cajal.[7–9] More recently, gain of function mutations of platelet-derived growth factor receptor alpha have been described in these tumors.[6]

Correspondence: Dr M Sabah, MRCPath, Department of Histopathology, Education and Research Centre, The Royal College of Surgeons in Ireland, Beaumont Hospital, Dublin 9, Ireland.
E-mail: munasabah@eircom.net
Received 22 March 2004; revised and accepted 4 May 2004; published online 4 June 2004

Clinically and pathologically, GISTs represent a spectrum of tumors that include benign, malignant and borderline variants. Prognostic features indicative of malignancy or high risk for aggressive clinical behavior are generally identified by increased tumor size and mitotic activity in the context of tumor location.[10,11] This lacks predictive accuracy which may be of increasing importance if the beneficial effect of the new tyrosine kinase inhibitor drug STI-571 (Gleevec) in the treatment of metastatic GISTs[12,13] expands the use of this new drug beyond metastatic GISTs to include nonmetastatic GISTs with high malignant potential.[10]

The aim of this study is to compare the frequency of loss of heterozygosity (LOH) of chromosome 9p in malignant and low-grade GISTs and to evaluate the expression of p16 protein in these two groups in order to ascertain the role if any of alterations in this region in malignant progression of GISTs, which might in turn provide an additional criterion for the selection of high-risk cases for treatment with STI-571.

Materials and methods

Tissue Samples and Pathological Analysis

A total of 21 samples of formalin-fixed paraffin-embedded tumor material were examined. There are different schemes for classification of GISTs. GISTs can be classified into very low risk, low risk,

intermediate risk and high risk, based on tumor size and mitotic count.[11,14] Alternatively, they have been classified according to site, size and mitotic activity into three categories: benign, malignant and uncertain or low malignant potential.[10] Using both of these systems, our cases fall into two groups: malignant (high risk) and low malignant potential (intermediate risk). There were nine primary malignant GISTs, four intra-abdominal recurrences and eight cases of low malignant potential GISTs. In two cases, the primary tumors (cases 13 and 16) and their recurrences (cases 18 and 21, respectively) were available for comparison. The tumors were subclassified according to their cellular pattern into spindle, epithelioid and mixed patterns (Table 1). Patients with low malignant potential tumors at the morphological level are alive and well with a mean follow-up period to date of 35 months (range 12–59 months).

Immunohistochemistry

All cases were positive for KIT to confirm the diagnosis of GIST. Antibodies to the following antigens were used: CD34, muscle-specific actin, smooth muscle actin, desmin, S100 protein and p16. Immunohistochemical detection was performed using the avidin-biotinylated peroxidase complex (Vectastain Elite ABC Kit; Vector Laboratories, Burlingame, CA, USA) with diaminobenzidine as the chromogen. Positive and negative controls were used in each staining run. For p16, the immunoreactivities were classified in accordance with previously published data[15] into three categories defined as follows: negative (−), less than 20% of cells were stained; heterogeneous, 20–80% were stained; positive (+), greater than 80% were stained. Samples showing either negative or heterogeneous staining were considered abnormal, whereas those with positive staining were interpreted as normal. The intensity of staining is not a component of this scoring system. The target antigen, clone, dilution and source are listed in Table 2.

DNA Microdissection

Two parallel 8 μm thick sections were dewaxed in xylene, rehydrated through various alcohol grades, rinsed well in distilled water and finally stained with hematoxylin.

Using the hematoxylin and eosin (HE) sections as a template, normal and tumor areas were microdissected under a stereomicroscope. Multiple areas of the tumor were sampled.

Genomic DNA Extraction

An amount of 60 μl of proteinase K solution (20 mg/ml proteinase K (Roche Diagnostics, Mannheim) in 50 mM Tris-HCl pH 7.4, 0.1 mM EDTA, 1% Tween) was added to normal and tumor tissue pellets, which were then digested at 55°C for 72 h.

PCR Amplification

Six fluorescent Cy5 end-labelled microsatellite markers that map to 9p region were used. Four markers map to 9p21; D9S916, D9S1814, D9S974 and D9S942. The latter two are within the coding sequence of *p16^{INK4A}*. D9S916 is telomeric to *p16^{INK4A}* and *p15^{INK4B}*, whereas D9S1814 is centromeric to *p15^{INK4B}*. D9S171 is at 9p13 (proximal to *p16^{INK4A}* and *p15^{INK4B}*). D9S230 is at 9p24.

PCR amplifications were performed in a final volume of 20 μl and consisted of 1 × PCR reaction buffer, 200 μM dNTPs, 1 mM $MgCl_2$ (Promega, Madison, WI, USA), 2 pmol of Cy5 labelled forward and reverse primers (TAGN, Newcastle) and 1 μl of sample DNA digest. After denaturation at 95°C for 5 min, 2 μl of *Taq* (1 U/μl) (Promega, Madison, WI, USA) were added at 80°C. A touchdown PCR was then carried out consisting of two cycles of 95°C for 1 min, 1 min at an initial annealing temperature (AT_I) (see Table 3), and 72°C for 1 min. Subsequent steps consisted of two cycles each with annealing temperature reduced by 2°C until 30 cycles were carried out at the final annealing temperature (AT_F°C). A final extension step at 72°C for 10 min completed the reactions. Following PCR, 5 μl PCR products mixed with agarose loading dye were electrophoresed through 12% polyacrylamide mini gels. The DNA fragments were visualized by ethidium bromide staining under ultraviolet light.

LOH Assay

The PCR products were diluted in distilled water, mixed with Cy5.5-labelled DNA size ladder and then analyzed on an OpenGene analyser (Visible Genetics, Toronto, Ontario). Allelic ratio in both normal and tumor samples were calculated and compared. The area under each peak, representing each allele in the microsatellite pair, was obtained using the GeneObjects Fragment Analysis Tool, and an allele deletion ratio was calculated by dividing the area under the larger peak by the area under the smaller peak in each of the normal and tumor DNA samples. A ratio of ratios between the normal and tumor PCR products was calculated to give an overall allele ratio. The cutoff value for LOH was 0.74 as was previously published from studies in our laboratory.[16]

In questionable cases, the PCR amplification and LOH analysis were repeated to ensure consistency in the results.

Modern Pathology (2004) 17, 1364–1371

Table 1 Clinical, histological and immunohistochemical findings

Case no.	*Age/(years) sex*	*Site*	*Maximum diameter (cm)*	*Mitoses/ 50 HPF*	*Necrosis*	*Cell type*	*Type*	*Follow-up (months)*	*KIT*	*CD34*	*Desmin*	*Smooth muscle actin*	*Muscle-specific actin*	*S100*	*p16*
1	63/M	Stomach	7	1	No	Spindle	LMP	12	+	+	−	−	−	−	+
2	53/F	Stomach	5	2	No	Spindle	LMP	31	+	+	−	−	−	−	+
3	57/M	Stomach	6	2	No	Epithelioid	LMP	22	+	+	−	−	±	−	+
4	93/M	Stomach	7	2	No	Epithelioid	LMP	42	+	+	−	±	−	−	+
5	81/F	Stomach	7	2	No	Mixed	LMP	45	+	−	−	−	−	−	+
6	19/F	Stomach	7	2	No	Spindle	LMP	39	+	−	−	−	−	−	+
7	55/F	Stomach	5	3	No	Spindle	LMP	59	+	+	−	−	−	−	+
8	59/F	Stomach	8.5	3	No	Mixed	LMP	30	+	+	−	+	+	−	+
9	49/F	Small intestine	10.5	2	No	Spindle	Malignant		+	−	+	+	+	−	−
10	50/F	Stomach	14	4	Yes	Epithelioid	Malignant		+	+	−	+	+	−	−
11	57/M	Small intestine	19	4	Yes	Spindle	Malignant		+	−	−	−	−	−	−
12	72/M	Stomach	20	6	Yes	Mixed	Malignant		+	+	−	−	−	−	−
13	43/F	Small intestine	9.5	10	Yes	Mixed	Malignant		+	+	−	−	−	±	−
14	69/F	Stomach	5.5	11	Yes	Epithelioid	Malignant		+	+	−	−	−	−	−
15	47/M	Stomach	7	20	Yes	Mixed	Malignant		+	+	−	−	−	−	−
16	71/M	Stomach	22.5	31	Yes	Epithelioid	Malignant		+	+	+	+	+	−	−
17	63/M	Stomach	7.5	70	Yes	Epithelioid	Malignant		+	−	+	+	+	±	−
18	47/F	Mesenteric deposits	Multiple nodules	6	No	Mixed	Recurrence		+	+	−	−	−	−	−
19	61/M	Mesenteric deposits	Multiple nodules	30	No	Mixed	Recurrence		+	−	−	±	−	−	−
20	50/M	Mesenteric deposits	Multiple nodules	35	Yes	Epithelioid	Recurrence		+	+	−	−	−	−	−
21	77/M	Mesenteric deposits	Multiple nodules	46	Yes	Epithelioid	Recurrence		+	+	−	−	−	−	−

F, female; M, male; +, positive staining; ±, focal staining; −, negative staining.

Results

Clinicopathological Features

Demographic data and histopathological features are summarized in Table 1. Eight cases were classified histologically as low malignant potential and nine cases were classified as malignant GISTs. There were 14 gastric, three small intestinal and four intra-abdominal mesenteric deposits. Histologically, six GISTs had a spindle cell pattern (Figure 1a), eight cases had an epithelioid morphology (Figure 1b) and seven cases showed a mixed cell pattern.

Immunohistochemical Features

As noted in the methodology, all cases were KIT positive and showed diffuse strong cytoplasmic and/or membranous staining (Figure 1c). In all, 15 cases (71%) were positive for CD34. Smooth muscle actin positive staining was present in seven cases (diffuse expression in five cases; focal expression in two cases), muscle-specific actin positive staining was observed in six cases (diffuse in five cases; focal in one case). Desmin-positive staining was present in three cases (14%). Focal positive staining for S100 was seen in two cases (10%).

Table 2 Clone, dilution and source of the antibodies used in the study

Antigen	*Clone*	*Dilution*	*Source*
KIT	Polyclonal	1/150	DAKO
CD34	QBEnd 10	1/40	DAKO
Muscle-specific actin	HHF35	1/3	Enzo
Smooth muscle actin	1A4	1/20 000	Sigma
Desmin	D33	1/100	DAKO
S100	Polyclonal	1/2000	DAKO
p16	16P07	1/100	NeoMarkers

All low malignant potential GISTs showed normal p16 expression with diffuse positive nuclear staining in more than 80% of tumor nuclei (Figure 1d). While intensity of staining is not a component in this scoring system for p16, it is of interest to note that cases with normal p16 expression showed moderate to strong staining. All malignant GISTs had absence of p16 staining (Figure 1e).

LOH Results

The average informative rate per marker was 67% (range from 52 to 90%). The LOH data are summarized in Figure 2. LOH was not identified in any of the low malignant potential cases. All malignant GISTs except one case (case 13) revealed LOH with at least one microsatellite marker. Intra-abdominal recurrent cases (18 and 21) showed more allelic deletions than their primary tumors (cases 13 and 16), respectively. Deletion at D9S974 was the most frequent deletion and was observed in all informative cases of malignant GISTs. Deletion at D9S942 was seen in 91% of informative cases. The other markers showed the following deletions with high-risk GISTs: D9S230, 67%; D9S916, 75%; D9S1814, 71%; D9S171, 56%. There was no correlation between histologic type, location and LOH findings.

Correlation of *p16^{INK4A}* Protein Expression and LOH Results

None of the eight p16-positive low malignant potential GISTs showed 9p21 LOH. All malignant cases with LOH showed absence of p16 immunostaining. However, case 13, which did not show any LOH at 9p, was negative for p16.

Table 3 Primer sequences and annealing temperatures used in touchdown PCR for each primer

Marker	*Primer sequence*	*Initial annealing temperature (AT_I°C)*	*Final annealing temperature (AT_F°C)*
D9S230	Forward 5′- acaggtcaccacccttcaac -3′ Reverse 5′- acaggagaagagctgaggca -3′	65	59
D9S916	Forward 5′- gatgtccagttgtcccttcataa -3′ Reverse 5′- atagactgccaaatttttggacc -3′	61	55
D9S974	Forward 5′- cctggtctggatcataaaatgaa -3′ Reverse 5′- tgtggaaattttctgtctggttc -3′	61	55
D9S942	Forward 5′- aagcaagattccaaacagtaaaca -3′ Reverse 5′- ttcgtttcacttttgagttttcc -3′	59	53
D9S1814	Forward 5′- tgtcagtggtatttacctttttgg -3′ Reverse 5′- cagaaggtcagtaggttcacagg -3′	61	55
D9S171	Forward 5′- agctaagtgaacctcatctctg -3′ Reverse 5′- tgattgttaataaagtagcccc -3′	59	53

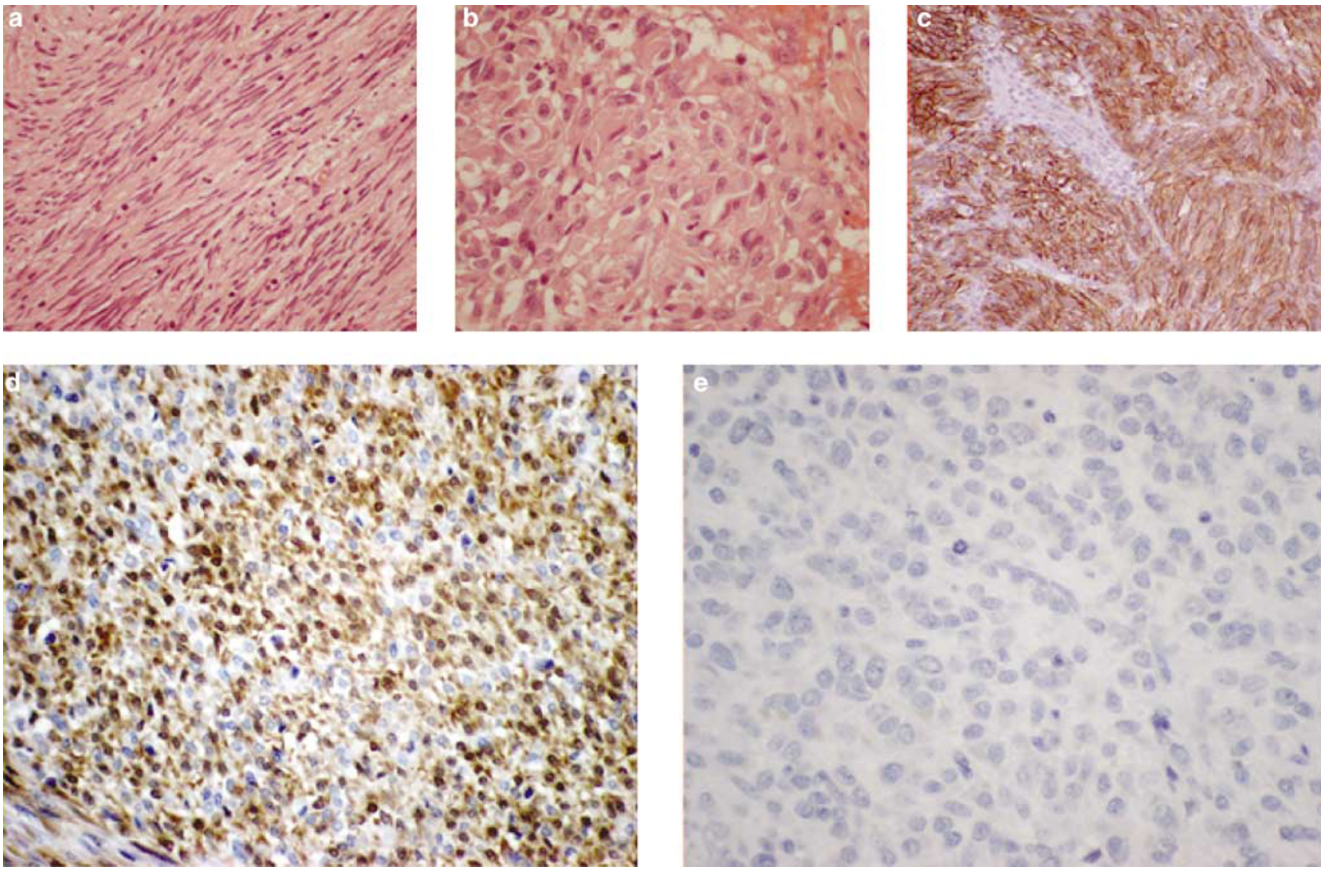

Figure 1 GIST with spindle (**a**) and epithelioid (**b**) cell patterns. Diffuse strong positive immunostaining with KIT (**c**). p16 expression in low malignant potential GIST (**d**). Negative p16 immunostaining in malignant GIST (**e**). Original magnification $\times 400$.

Discussion

In this study, we examined a series of 21 GISTs by immunohistochemical stains for p16 and LOH of chromosome 9p. All the cases were positive for KIT and 71% of cases were positive for CD34. CD34 and KIT protein have been shown to be markers of the interstitial cells of Cajal.[4] Our results are concordant with those reported by Kindblom *et al*[4] in a study of 78 GISTs. Immunoreactivity for KIT was seen in all cases and 56 (72%) showed coexpression of CD34.

The majority of GISTs have activating mutations of KIT or platelet-derived growth factor receptor alpha, which result in activation of signal transduction pathways and therefore are critical steps in initiating oncogenic events in most GISTs and can be targeted by STI-571.[6] Certain chromosomal aberrations in GISTs appear to be secondary alterations. For example, loss of chromosomes 14 and 22 are common to GISTs irrespective of site, differentiation and clinical behavior and have been reported to benign, borderline and malignant GISTs,[17–21] suggesting that these changes are early events in GIST tumorigenesis.

On the other hand, structural rearrangement of chromosome 1 is thought to represent a secondary change in progression and malignant transformation of GISTs.[20,22–24]

Using interface fluorescent *in situ* hybridization, Debiec-Rychter *et al*[22] analyzed 14 malignant, two intra-abdominal recurrent and nine benign GISTs. Loss of chromosomes 1, 9 and 15 were the only recurrent numerical changes seen exclusively in malignant GISTs.[22]

Consistent loss of chromosome 9p has also been documented in malignant GISTs by comparative genomic hybridization-based studies.[18,25] Gunawan *et al*[18] studied 19 GISTs (five low risk, 11 high risk and three recurrences). The authors reported loss of 9p in five of six patients with clinically aggressive behavior including two recurrent and three metastasizing GISTs, and these were absent in the low-risk group.[18] Similarly, El-Rifai *et al*[25] examined 95 GISTs (24 benign, 36 malignant and 35 metastatic). Losses of 9p were found to be highly specific for malignant and metastatic GISTs and were never seen in benign tumors.[25]

Studies based on LOH have the advantage over comparative genomic hybridization studies of identifying small deletions.[26]

LOH of chromosome 9p has been detected in many primary human tumors and cell lines.[27] This

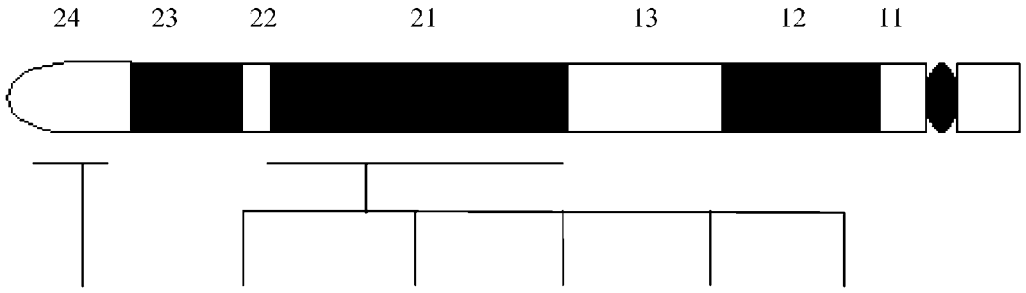

Case No.	D9S230	D9S916	D9S974	D9S942	D9S1814	D9S171
1	⊘	○	○	○	○	⊘
2	○	○	⊘	○	⊘	⊘
3	⊘	○	⊘	○	⊘	⊘
4	⊘	○	○	○	⊘	○
5	○	○	○	○	○	○
6	⊘	○	○	○	○	○
7	⊘	○	⊘	○	○	○
8	⊘	○	○	○	○	○
9	○	●	●	●	○	●
10	○	⊘	⊘	●	⊘	○
11	●	●	⊘	●	⊘	●
12	●	⊘	⊘	●	⊘	●
13	○	○	⊘	○	○	○
14	●	●	●	●	●	●
15	⊘	⊘	●	●	⊘	⊘
16	●	⊘	●	⊘	●	○
17	⊘	●	⊘	●	⊘	⊘
18	●	○	⊘	●	●	○
19	⊘	●	●	●	⊘	⊘
20	⊘	●	●	●	●	⊘
21	●	⊘	●	⊘	●	●

Figure 2 Microsatellite map of LOH of 9p, with tabulated results: ●, indicates LOH; ○, indicates no LOH; ⊘, uninformative (homozygosity).

chromosomal region harbors *p15*^{INK4B}[27,28] and *p16*^{INK4A},[29,30] which are likely candidates for tumor suppressor genes since they encode nuclear proteins that have been shown to block cell cycle progression at the G1/S transition by their ability to interfere with the catalytic activity of cyclin D/CDK4 complexes.[30]

LOH analysis was performed in this study by using six microsatellite markers at the 9p region. Four markers map to 9p21; D9S916, D9S1814, D9S974 and D9S942. The latter two are within the coding sequence of *p16*^{INK4A}. D9S171 is at 9p13 (proximal to *p16*^{INK4A} and *p15*^{INK4B}). D9S230 is at 9p24. Deletion at D9S974 was seen in all informa-

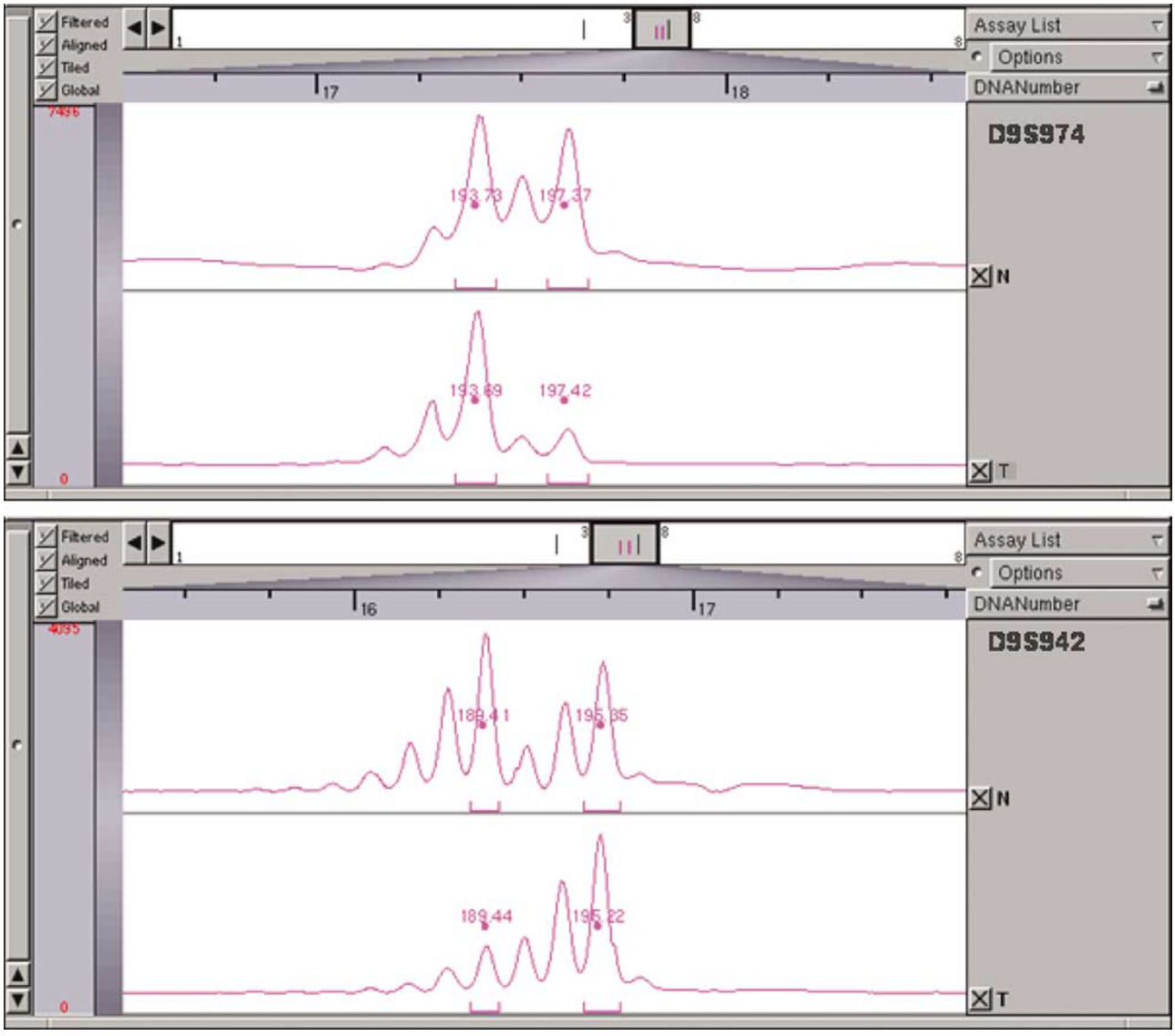

Figure 3 LOH at D9S974 and D9S942.

tive cases of malignant GISTs, followed by deletion at D9S942 (Figure 3). These results suggest that deletion of *p16*^{INK4A} may play a role in the pathogenesis/transformation of malignant GISTs.

Little is known about *p16*^{INK4A} alteration in GISTs. Schneider-Stock *et al*[31] reported that *p16*^{INK4A} alteration was detected in benign, borderline and malignant GISTs but nevertheless was considered as an independent poor prognostic factor. The apparent discrepancy with our findings may relate to the difference in classification methods. It is clear that some of the tumors classified in their study as borderline GIST with *p16*^{INK4A} alteration would be classified in this study as malignant GISTs (on the bases of the location, tumor size and mitotic count). However, the authors used different GIST classification and did not take the site of the tumor into consideration. Furthermore, the criteria used for detection of p16 immunoreactivity were different from those used in this study and other studies.[15] This might explain some of the discrepancy encountered in that study between *p16*^{INK4A} alteration and p16 protein expression.

Kim *et al*[21] analyzed 14 GISTs (two benign, seven borderline and five malignant). Homozygous deletion on chromosome 9p was absent in benign and borderline cases but was present in two malignant cases.[21]

Our LOH results are in keeping with those reported in the literature. Strong correlation between immunohistochemical expression and LOH at 9p21 is present. Only one malignant case (case 13) showed absence of p16 immunostaining without the presence of LOH. There are three possible explanations: (1) technical flaw in LOH study. (2) p16 immunoreactivity is a reflection of other genetic or epigenetic changes including DNA methylation and post-translational modification that are not

detectable by LOH. And (3) The case was homozygous for D9S974 marker, therefore was not informative. LOH at this marker was detected in all informative malignant cases studied. Given the uniformity of the result, the last explanation seems most likely.

Whether borderline GISTs are precursors of malignant GISTs that accumulate genetic alteration during malignant transformation or whether they represent a biologically indolent and distinct subset of GISTs is still uncertain. Our results support other observations in the literature and suggest that genetic alterations in malignant GISTs are distinct from borderline tumors and that LOH on chromosome 9 and p16 immunostaining may be used as complementary tools for the prognostication of GISTs.

References

1 O'Leary T, Berman JJ. Gastrointestinal stromal tumors: answers and questions. Hum Pathol 2002;33:456–458.
2 Hjermstad BM, Sobin LH, Helwig EB. Stromal tumors of the gastrointestinal tract: myogenic or neurogenic? Am J Surg Pathol 1987;11:383–386.
3 Rubin BP, Fletcher JA, Fletcher CD. Molecular insights into the histogenesis and pathogenesis of gastrointestinal stromal tumors. Int J Surg Pathol 2000;8:5–10.
4 Kindblom LG, Remotti HE, Aldenborg F, *et al.* Gastrointestinal pacemaker cell tumor (GIPACT): gastrointestinal stromal tumors show phenotypic characteristics of the interstitial cells of Cajal. Am J Pathol 1998;152:1259–1269.
5 Heinrich MC, Rubin BP, Longley BJ, *et al.* Biology and genetic aspects of gastrointestinal stromal tumors: KIT activation and cytogenetic alterations. Hum Pathol 2002;33:484–495.
6 Heinrich MC, Corless CL, Demetri GD, *et al.* Kinase mutations and imatinib response in patients with metastatic gastrointestinal stromal tumor. J Clin Oncol 2003;21:4342–4349.
7 Vliagoftis H, Worobec AS, Metcalfe DD. The proto-oncogene c-kit and c-kit ligand in human disease. J Allergy Clin Immunol 1997;100:435–440.
8 Sarlomo-Rikala M, Kovatich AJ, Barusevicius A, *et al.* CD117: a sensitive marker for gastrointestinal stromal tumors that is more specific than CD34. Mod Pathol 1998;11:728–734.
9 Miettinen M, Sarlomo-Rikala M, Lasota J. Gastrointestinal stromal tumors: recent advances in understanding of their biology. Hum Pathol 1999;30:1213–1220.
10 Miettinen M, El Rifai W, Sobin HL, *et al.* Evaluation of malignancy and prognosis of gastrointestinal stromal tumors: a review. Hum Pathol 2002;33:478–483.
11 Fletcher CD, Berman JJ, Corless C, *et al.* Diagnosis of gastrointestinal stromal tumors: a consensus approach. Hum Pathol 2002;33:459–465.
12 Joensuu H, Roberts PJ, Sarlomo-Rikala M, *et al.* Effect of the tyrosine kinase inhibitor STI571 in a patient with a metastatic gastrointestinal stromal tumor. N Engl J Med 2001;344:1052–1056.
13 van Oosterom AT, Judson I, Verweij J, *et al.* Safety and efficacy of imatinib (STI571) in metastatic gastrointestinal stromal tumours: a phase I study. Lancet 2001;358:1421–1423.
14 Fletcher CD, Berman JJ, Corless C, *et al.* Diagnosis of gastrointestinal stromal tumors: a consensus approach. Int J Surg Pathol 2002;10:81–89.
15 Yoo J, Park SY, Kang SJ, *et al.* Altered expression of G1 regulatory proteins in human soft tissue sarcomas. Arch Pathol Lab Med 2002;126:567–573.
16 Butler D, Collins C, Mabruk M, *et al.* Deletion of the FHIT gene in neoplastic and invasive cervical lesions is related to high-risk HPV infection but is independent of histopathological features. J Pathol 2000; 192:502–510.
17 El Rifai W, Sarlomo-Rikala M, Miettinen M, *et al.* DNA copy number losses in chromosome 14: an early change in gastrointestinal stromal tumors. Cancer Res 1996;56:3230–3233.
18 Gunawan B, Bergmann F, Hoer J, *et al.* Biological and clinical significance of cytogenetic abnormalities in low-risk and high-risk gastrointestinal stromal tumors. Hum Pathol 2002;33:316–321.
19 Sandberg AA, Bridge JA. Updates on the cytogenetics and molecular genetics of bone and soft tissue tumors. Gastrointestinal stromal tumors. Cancer Genet Cytogenet 2002;135:1–22.
20 Breiner JA, Meis-Kindblom J, Kindblom LG, *et al.* Loss of 14q and 22q in gastrointestinal stromal tumors (pacemaker cell tumors). Cancer Genet Cytogenet 2000;120:111–116.
21 Kim NG, Kim JJ, Ahn JY, *et al.* Putative chromosomal deletions on 9p, 9q and 22q occur preferentially in malignant gastrointestinal stromal tumors. Int J Cancer 2000;85:633–638.
22 Debiec-Rychter M, Lasota J, Sarlomo-Rikala M, *et al.* Chromosomal aberrations in malignant gastrointestinal stromal tumors: correlation with c-KIT gene mutation. Cancer Genet Cytogenet 2001;128:24–30.
23 O'Leary T, Ernst S, Przygodzki R, *et al.* Loss of heterozygosity at 1p36 predicts poor prognosis in gastrointestinal stromal/smooth muscle tumors. Lab Invest 1999;79:1461–1467.
24 Derre J, Lagace R, Terrier P, *et al.* Consistent DNA losses on the short arm of chromosome 1 in a series of malignant gastrointestinal stromal tumors. Cancer Genet Cytogenet 2001;127:30–33.
25 El Rifai W, Sarlomo-Rikala M, Andersson LC, *et al.* DNA sequence copy number changes in gastrointestinal stromal tumors: tumor progression and prognostic significance. Cancer Res 2000;60: 3899–3903.
26 Dib C, Faure S, Fizames C, *et al.* A comprehensive genetic map of the human genome based on 5,264 microsatellites. Nature 1996;380:152–154.
27 Nobori T, Miura K, Wu DJ, *et al.* Deletions of the cyclin-dependent kinase-4 inhibitor gene in multiple human cancers. Nature 1994;368:753–756.
28 Hannon GJ, Beach D. p15INK4B is a potential effector of TGF-beta-induced cell cycle arrest. Nature 1994; 371:257–261.
29 Kamb A, Gruis NA, Weaver-Feldhaus J, *et al.* A cell cycle regulator potentially involved in genesis of many tumor types. Science 1994;264:436–440.
30 Serrano M, Hannon GJ, Beach D. A new regulatory motif in cell-cycle control causing specific inhibition of cyclin D/CDK4. Nature 1993;366:704–707.
31 Schneider-Stock R, Boltze C, Lasota J, *et al.* High prognostic value of p16INK4 alterations in gastrointestinal stromal tumors. J Clin Oncol 2003;21: 1688–1697.